Cooperative Effects in the Binding of Substrates to Nickel(II) and Nickel(III) Complexes with a Bis(macrocyclic) Ligand

Peter Comba,*[a] Yaroslaw D. Lampeka,*[b] Alexander Y. Nazarenko,[c] Alexander I. Prikhod'ko,[b] Hans Pritzkow,[a] and Joanna Taraszewska[d]

Keywords: Template reaction / Spin equilibrium / Recognition / Cooperative effects / Nickel / N ligands

Nickel(II) complexes of mono- and bis(macrocyclic) ligands are the products of a nickel(II)-assisted template reaction with 2,3,2-tet, melamine and formaldehyde [2,3,2-tet = bis–*N*,*N*′-(2-aminoethyl)propane-1,3-diamine; melamine = 2,4,6-triamino-1,3,5-triazine]. The structures of two four-coordinate, diamagnetic nickel(II) complexes (protonated and non-protonated form) and of a six-coordinated paramagnetic nickel(II) compound with the protonated ligand have been determined by X-ray crystallography. Electronic spectroscopy was used to analyze the equilibrium between the paramagnetic and diamagnetic forms, and the electrochemical properties have been studied extensively ($Ni^{III/II}$ and $Ni^{II/I}$ couples). The equilibrium between the paramagnetic and diamagnetic forms and the nickel(III/II) couple are strongly dependent on the electrolyte, and sulfate is found to be coordinated selectively to the apical positions of both the nickel(II) and nickel(III) centers of the dinuclear compound. The structural, thermodynamic and electrochemical studies suggest that cooperative effects, involving coordination of sulfate to one nickel center, assisted by hydrogen bonding to an axially coordinated water molecule of the other nickel center, is responsible for the recognition of this anion.

Introduction

Mannich-type, metal-ion-assisted condensation reactions of *cis*-disposed primary amines with formaldehyde and a nucleophile have been used extensively to prepare hexaamine cages, pendent-arm macrocyclic and open-chain ligands with N-, S-, Se- and O-donors, coordinated to copper, nickel, palladium, cobalt and a few other metal centers.[1−6] Due to the rigidity of the aromatic spacer groups and the possibility to obtain oligonuclear complexes in one-pot reactions, aromatic amines, melamine in particular (melamine = 2,4,6-triamino-1,3,5-triazine), are of interest as "capping" groups in metal-based template condensations. However, in the copper(II)-assisted condensation the poor nucleophilicity of the aniline-type amines results in low yields of the desired mono-, bis- and tris(macrocyclic) products,[7−9] and this is also the case for the nickel(II)-assisted Mannich reaction (see below). When the mono-(macrocyclic), melamine-substituted nickel(II) or copper(II) intermediates are used as capping groups in the template reactions mixed-metal oligonuclear systems may be obtained.[10]

The two factors which make the melamine-based oligomacrocyclic ligand complexes of particular interest are vacant or labile axial sites at the metal centers, with the possibility for cooperative binding and activation of substrates in the bis- and tris(macrocyclic) ligand systems, and the fact that melamine can be protonated. π-Stacking, hydrogen bonding and bonding to relatively labile axial sites of transition metal complexes have been described as important features for host-guest interactions.[11−16] Metal complex hosts which have been reported include trizinc(II) compounds and a tetrahedral tetragallium(III) complex.[17−19] A variety of possible applications, including crystal engineering, the preparation and stabilization of anionic metal complexes, as well as cooperativity and selectivity of anion binding have been described with melamine-based macrocyclic ligand complexes.[7−9,20]

Here, we present details on the syntheses and structures of nickel(II) complexes with melamine-based mono- and

[a] Universität Heidelberg, Anorganisch-Chemisches Institut, Im Neuenheimer Feld 270, 69120 Heidelberg, Germany
Fax: (internat.) + 49-(0)6221/546617
E-mail: comba@akcomba.oci.uni-heidelberg.de
[b] L. V. Pisarzhevsky Institute of Physical Chemistry, National Academy of Science of the Ukraine, Prospekt Nauki 31, 03039 Kiev 39, Ukraine
Fax: (internat.) + 38-044/2656216
E-mail: ditop@iphch.kiev.ua
[c] Department of Chemistry, State University of New York, College at Buffalo, 1300 Elmwood Ave, Buffalo, NY 14222-1095, USA
[d] Institute of Physical Chemistry, Polish Academy of Sciences, Kasprzaka 44/52, 01-224 Warsaw, Poland
Supporting information for this article is available on the WWW under http://www.eurjic.com or from the author.

bis(macrocyclic) ligands and a thorough study of the equilibria between the paramagnetic and diamagnetic forms and electrochemical reduction and oxidation processes; this leads to a detailed understanding of the importance of cooperative effects in the recognition of sulfate by the dinickel(II) and the dinickel(III) complexes.

Results and Discussion

Synthesis

The macrocyclization reaction of the open-chain copper(II) complex $[Cu(2,3,2\text{-tet})]^{2+}$ with formaldehyde and melamine yields three possible compounds of different nuclearity, $[Cu(L^1)]^{2+}$, $[Cu_2(L^2)]^{4+}$ and $[Cu_3(L^3)]^{6+}$ (Scheme 1).[7−9] Only complexes with the mono- and bis(macrocyclic) ligands, $[Ni(L^1)]^{2+}$ and $[Ni_2(L^2)]^{4+}$, can be isolated with $[Ni(2,3,2\text{-tet})]^{2+}$ as the template. These are separated by column chromatography, using 0.2 mol·L^{-1} and 0.4 mol·L^{-1} aqueous $NaClO_4$ as eluents. Melamine generally leads to lower yields of the macrocyclic ligand products than other locking groups in metal-ion-assisted Mannich condensations. The yields of the copper(II) complexes are 9%, 13% and 7% for the mono-, bis- and tris(macrocyclic) ligand complexes, respectively.[7−9] The yields of the nickel(II) compounds are even lower (see Exp. Sect.).

An aromatic nitrogen atom of melamine in $[M(L^1)]^{2+}$ and $[M_2(L^2)]^{4+}$ can be protonated (pK_{a1} = 4.2 for $[Cu(L^1)]^{2+}$ [7]). The resulting sites for hydrogen bonding are of importance for the stabilization of specific types of arrangements of the macrocyclic cations in the crystal lattices.[7−9,20]) However, since protonation does not result in significant changes of the solution spectroscopic and electrochemical properties of the nickel compounds (see below), we conclude that protonation alone does not lead to stable supramolecular assemblies in solution, similar to those observed in crystal lattices.

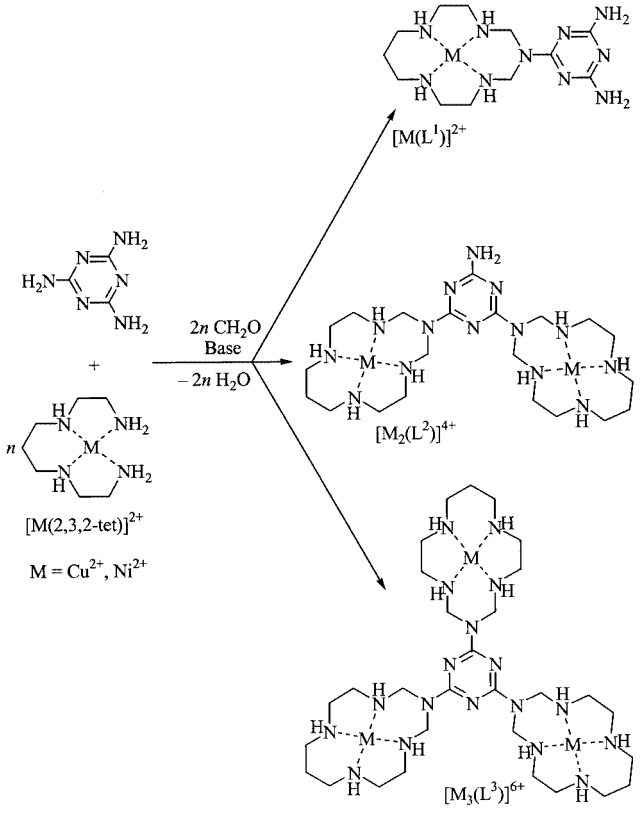

Scheme 1

Vibrational spectra of the complexes have features, which are characteristic for both the melamine fragment and the tetraazamacrocyclic ligand nickel(II) core. Similar to the copper(II) compounds,[9] the number of transitions which correspond to the out-of-plane vibrations of the aromatic amino groups [$\delta(NH_2)$, 1660 cm^{-1} in melamine] are related to the nuclearity of the complexes and, for complexes of L^1 and L^2, to the degree of protonation of the melamine fragment: three bands (1700, 1650, 1600 cm^{-1}) are observed in the nickel(II) compounds of the protonated mono(macrocyclic) ligand $(HL^1)^+$; two bands (1667 and 1600 cm^{-1}) are characteristic for complexes of the protonated bis(macrocyclic) ligand $(HL^2)^+$; one band is observed for complexes of the free bases ($[Ni(L^1)]^{2+}$, 1600 cm^{-1}; $[Ni_2(L^2)]^{4+}$, 1610 cm^{-1}).

Molecular and Crystal Structures

The structures of the mono(macrocyclic) ligand nickel(II) complexes with the non- and monoprotonated melamine fragment and diamagnetic or paramagnetic nickel(II) centers, i.e., four-coordinate nickel(II) complexes of two forms of L^1, $[Ni(L^1)](ClO_4)_2\cdot H_2O$ (**1**) and $[Ni(HL^1)](ClO_4)_2\text{-}Cl\cdot H_2O$ (**2**), and the six-coordinate complex of $(HL^1)^+$ $[Ni(HL^1)(OSO_3)(OH_2)]ClO_4\cdot 5H_2O$ (**3**) were determined by X-ray crystallography. Single crystals of the four-coordinate dinickel(II) compound $[Ni_2(L^2)](ClO_4)_4\cdot 2H_2O$ (**4**) were also obtained but were of poor quality, the preliminary data obtained were used to determine the overall conformation of the dinuclear cation. The variety of the structural data, together with the published structures of the corresponding copper(II) compounds, i.e., $[Cu(L^1)(OClO_3)_2]\cdot H_2O$ (**5**)[9] and **6**,[20] $[Cu(HL^1)(OClO_3)_2](ClO_4)\cdot H_2O$ (**7**),[9] $[Cu(HL^1)\text{-}(OClO_3)](ClO_4)_2\cdot 2H_2O$ (**8**),[7] and $\{[Cu(HL^1)(OH_2)(Cl)]\text{-}[Cu(HL^1)(OClO_3)(Cl)]\}(ClO_4)_3$ (**9**),[9] form a broad basis for a comparative analysis of the molecular and crystal structures of melamine-based macrocyclic ligand complexes [copper(II) compounds of L^2 and L^3, which have also been reported before [8,9] are not included in this analysis].

Molecular Structures

The geometries of the macrocyclic ligands L^1 and $(HL^1)^+$ in the nickel(II) complexes (Figure 1) and in the corresponding copper(II) compounds [7−9,20] are identical, i.e., *trans*-III (*RRSS*).[21] The distances and angles are typical for nickel(II) [and copper(II)] complexes of 14-membered tetraaza macrocycles.[22] The melamine rings are nearly planar (rms 0.01−0.02 Å), as observed in other 1,3,5-triazine derivatives.[23] The nickel(II) ions in **1** and **2** are coordinated in a planar chromophore to four nitrogen donors of

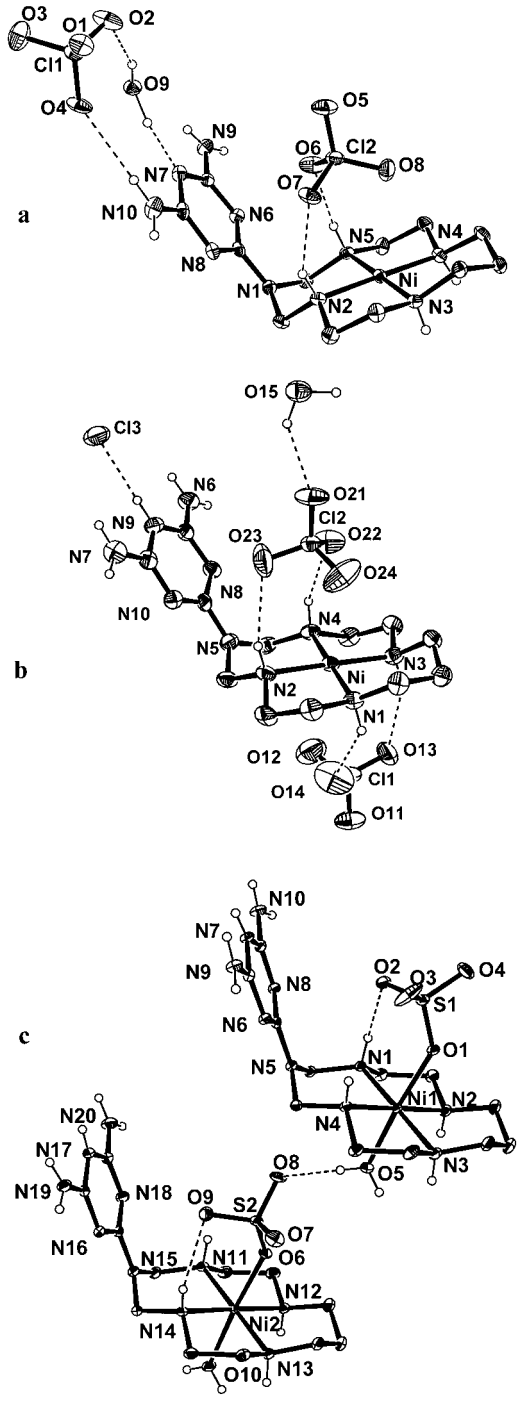

Figure 1. ORTEP[40] view (30% probability ellipsoids) of **1** (a), **2** (b) and **3** (c); C−H hydrogen atoms are omitted for clarity; selected hydrogen bond lengths are: **1**: O(4)···H−N(10) 3.278 Å, O(9)−H···O(2) 2.956 Å, O(9)−H···N(7) 2.747 Å, N(2)−H···O(7) 3.008 Å, N(5)−H···O(6) 3.047 Å; **2**: N(1)−H···O(14) 2.984 Å, N(3)−H···O(13) 3.116 Å, N(2)−H···O(23) 3.148 Å, N(4)−H···O(22) 3.071 Å, Cl(3)···H−N(9) 2.988 Å; **3**: O(5)−H···O(8) 2.680 Å, O(10)−H···O(4′) 2.630 Å O(2)···H−N(1) 2.938 Å; O(9)···H−N(14) 3.010 Å

the macrocycle with nearly identical metal−nitrogen distances, as expected for four-coordinate, diamagnetic nickel(II) compounds[22] (see Table 1). The paramagnetic nickel(II) ion in **3** is six-coordinate, with a sulfate anion and a water molecule completing the coordination sphere, in a nearly regular octahedral geometry with significantly longer metal−donor distances than observed in **1** and **2** (see Table 1).

From the structural parameters of the complexes of L^1 (see Table 1), it emerges that four-, five- or six-coordinate metal ions with a variety of metal donor distances [Ni−N < 1.95 Å in diamagnetic nickel(II); Cu−N ≈ 2.02 Å; Ni−N > 2.06 Å in paramagnetic nickel(II) complexes, 2.1 Å $<$ M−O^{ax} < 2.6 Å] are well accommodated in the macrocycle in *trans*-III configuration, with close to planar MN_4 chromophores and the expected N−M−N bite angles (ca. 95° for the six-membered and ca. 85° for the five-membered chelate rings). The flexibility in the orientation of the melamine rings with respect to the mean MN_4 planes (angles α, β, γ, see Figure 2) allows for a wide range of substrates to be stabilized (this is of specific importance for the bis- and tris(macrocyclic) compounds, see ref.[9]) and for the stabilization of specific crystal lattice patterns (see below).

In complexes with two or three macrocyclic ligands fixed on the melamine spacer group, as in L^2 and L^3, there are two possible conformations (*syn* or *anti* in L^2; *syn*,*syn* or *syn*,*anti* in L^3). Both are similar in energy[8,9] and the preference for a particular structure in a crystal lattice or in solution is a function of the substrates (or electrolytes) and the environment (lattice or solvent). Both structural types have been observed for $[Cu_3(L^3)]^{6+}$,[8,9] only the *anti* isomer was characterized structurally for the copper(II) complex with the bis(macrocyclic) ligand,[9] and the same is observed in the corresponding dinickel(II) system **4** discussed here. Also, host-guest complexation studies and preliminary computations indicate that the barrier for isomer interconversion (*syn*/*anti*) is relatively low.[9,24] The experimental structural data support this assumption (angles α, β, γ, see Table 1); there appears to be a large flexibility (shallow energy minimum) with an optimum structure of $10° < \alpha < 30°$ [planarity of the pendent amine groups of melamine would require $\alpha = 0°$, values of $\alpha > 2°$ have been observed in copper(II) complexes[9]], $70° < \beta < 90°$ and $40° < \gamma < 60°$. This flexibility is an advantage for the cooperative binding and activation of substrates at the axial sites of the metal chromophores.

Crystal Packing

Three main structural motifs have been found in crystal lattices of copper(II) complexes with the melamine-derived mono(macrocyclic) ligand,[7,9,20] i.e., infinite tapes of the molecular cations (hydrogen bonds between the free amino groups of the melamine substituents and water molecules or perchlorate anions, 5.0 Å $< d_2 <$ 5.7 Å, see Figure 3, Table 2), π-stacking interactions between the melamine rings, $d_4 \approx 3.5$ Å, $\delta \approx 0°$ (δ is the angle between the two melamine ring planes), and, for the copper(II) complexes **5** and **6** with the free-base ligand, the formation of double-stranded tapes, due to hydrogen bonding between self-complementary melamine groups (ADA, acceptor-donor-acceptor pattern). Two different types of stacked pairs are possible, depending on the orientation of the macrocyclic

Table 1. Structural parameters (distances in Å, angles in °) of metal(II) complexes with the melamine-derived macrocyclic ligand L^1

Complex	Structure of the chromophore							Conformation of the melamine macrocycle fragments[a]		
	Equatorial M−N	Axial M−O	N−M−N (av. 6-membered chelate ring)	N−M−N (av. 5-membered chelate ring)	Rms of MN_4	Deviation of M from MN_4 plane	θ[b]	α	β	γ
Non-protonated ligand L^1										
Ni (**1**)	1.936−1.943	none	94.2 ± 0.2	85.8 ± 0.2	0.01	0.01	1.1	27.2	86.2	58.6
Cu (**5**)[9]	2.015−2.025	2.458, 2.628 (ClO_4)	94.2 ± 0.4	85.7 ± 0.0	0.03	0.05	5.3	23.0	70.7	45.5
Cu (**6**)[20]	2.009−2.026	2.511, 2.617 (ClO_4)	94.3 ± 0.3	85.6 ± 0.3	0.03	0.04	4.4	12.2	80.4	36.9
Protonated ligand $(HL^1)^+$										
Ni (**2**)	1.921−1.939	none	93.3 ± 1.7	86.7 ± 0.3	0.02	0.02	2.7	11.3	86.9	48.5
Cu (**7**)[9]	2.013−2.029	2.585, 2.594 (ClO_4)	94.9 ± 2.6	85.0 ± 0.0	0.01	0.01	2.2	18.9	82.5	61.6
Cu (**8**)[7] [c]	2.008−2.019,	2.521 (H_2O)	94.8 ± 0.5,	85.1 ± 0.3,	0.01,	0.01,	1.7,	12.0,	89.1,	44.7
	2.006−2.052	none	94.7 ± 0.6	85.2 ± 0.1	0.03	0.05	5.6	12.4	86.4	46.7
Coordinated substrate, protonated ligand $(HL^1)^+$										
Ni (**3**)[c]	2.064−2.081,	2.099 (SO_4), 2.135 (H_2O)	94.6 ± 0.8,	85.4 ± 0.2,	0.01,	0.01,	1.0,	10.1,	86.7,	45.9
	2.062−2.079	2.090 (SO_4), 2.135 (H_2O)	94.6 ± 0.3	85.4 ± 0.2	0.01	0.02	1.8	12.3	86.9	46.9
Cu (**9**)[9] [c]	2.011−2.028,	2.718 (H_2O), 2.826 (Cl),	94.1 ± 3.3,	85.6 ± 0.1,	0.04,	0.04,	7.8,	9.9,	88.8,	52.3
	2.016−2.023	2.660 (Cl), 2.808 (ClO_4)	94.4 ± 2.7	85.0 ± 0.1	0.06	0.12	11.8	9.6	88.5	49.9

[a] For definition of the angles see Figure 2. [b] Average angle between two N−M−N planes (tetrahedral or pyramidal distortion of the chromophore). [c] Two independent molecules in the asymmetric unit.

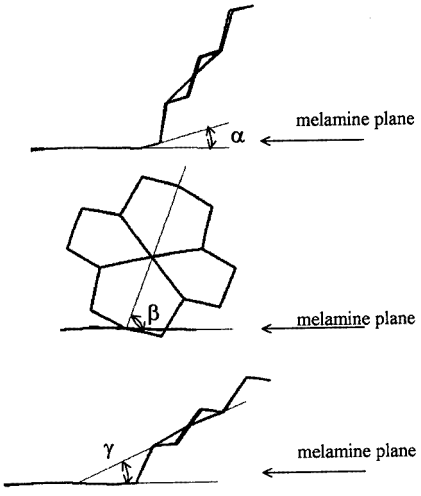

Figure 2. Definition of the structural parameters used for the analysis of the geometry of the melamine macrocycle fragments

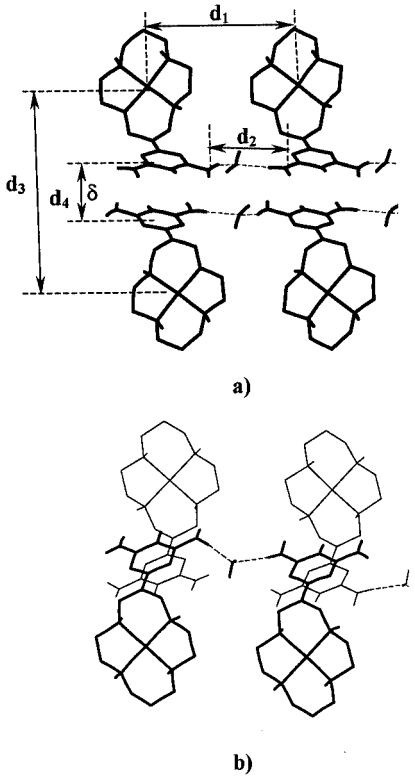

Figure 3. The two different types of stacked pairs of $[M(L^1)]^{n+}$ complexes

rings with respect to the neighboring melamine plane (see Figure 3a,b). The relevant structural parameters are given in Table 2, see Figure 3 for their definition.

Interestingly, in the crystal lattice of **1** the common features of all other structures are absent (see Figure 4a). This presumably is due to the specific location of a water molecule relative to the melamine residues; the hydrogen bonding patterns (see Figure 1a) do not allow the formation of the usual tapes and prevent a complementary hydrogen bonding interaction between pairs of melamine rings. Also, this indicates that the formation of the usually observed tapes, stabilized by hydrogen bonding and π-stacking, is, as expected, a relatively small contribution which may be overcome by other effects.

Similar to the copper(II) complexes **5**−**8**,[7,9,20] the macrocyclic cations in the crystal lattice of **2** form infinite hydrogen-bonded chains, bridged by water molecules and supported by π-interactions between the parallel and nearly coaxial melamine rings (see b in Figure 4). The metal−metal distance d_1 is slightly shorter than in the copper(II) analogues, and d_2 is intermediate between those observed in the copper(II) compounds.

Table 2. Structural parameters (distances in Å, angles in °) related to the crystal packing of complexes with the melamine-derived mono(macrocyclic) ligand

Complex	Tapes			Stacks		
	d_1	d_2	N−H···O(H_2O)	d_3	d_4	δ
Non-protonated ligand L^1						
Ni (**1**)	10.87	6.36	no H-bonds	no π-stacking		
Cu (**5**)[9]	9.54	5.11	2.86, 2.87	11.61	3.5	0
Cu (**6**)[20]	10.00	5.66	2.99, 3.05	11.64	3.5	0
Protonated ligand $(HL^1)^+$						
Ni (**2**)	9.43	4.81	2.91, 2.93	12.29	3.2	0
Cu (**7**)[9]	9.58	5.00	2.89, 2.95	13.00	av. 3.4	1.6
Cu (**8**)[7]	9.49	4.89	2.90, 3.00	12.64	3.5	0
Ni (**3**)	9.12; 9.32	4.82; 4.79	2.81, 2.96; no H-bonds	11.17;[a] 12.26;[b] 12.32[b]	av.4.2; 4.5; 4.5	4.9; 0; 0
Cu (**9**)[9]	9.67	5.10	3.01, 3.08[c]	11.28[b]	av.3.6	5.6

[a] "Open" stack (see Figure 3a). [b] "Closed" stack (see Figure 3b). [c] Bridging perchlorate anion instead of water molecule.

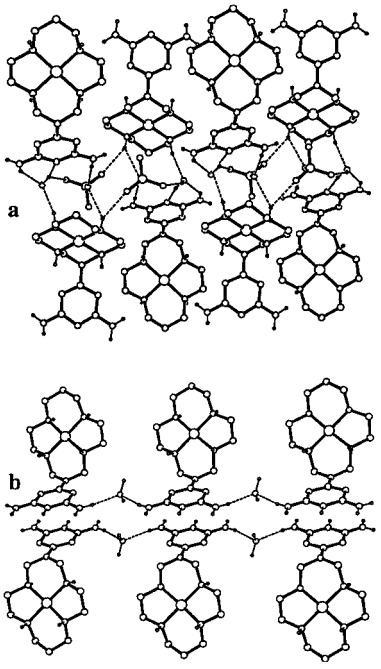

Figure 4. Crystal packing of **1** with intermolecular hydrogen bonds (a) and π-stacked cationic tapes in the crystal lattice of **2** (b)

The crystal lattice of **3** is unique, the tape structure has a "stair"-type arrangement (see a in Figure 5). This is due to the water molecule $H_2O(27)$, which not only bridges two neighboring cations in the tape but also forms a hydrogen bond to the aromatic nitrogen atom of the adjacent tape [O(27)−H···N(8), 2.988 Å]. In addition, the tape observed in **3** is not isotropic and consists of distinct hydrogen-bound dimers (d_1 = 9.32 Å, d'_1 = 9.12 Å); the distance between the melamine amino groups of the non-bonded adjacent cations is smaller than for those connected by hydrogen bonds (see Table 2). This tape interacts via π-stacking with another tape of the same structure but shifted by one macrocyclic unit, i.e., alternating hydrogen bonds hold the two tapes together (see b in Figure 5).

The melamine substituents in all examples form π-stacked pairs of cations; generally, the metal chromophores of the stacked cations are oriented at different sides of the

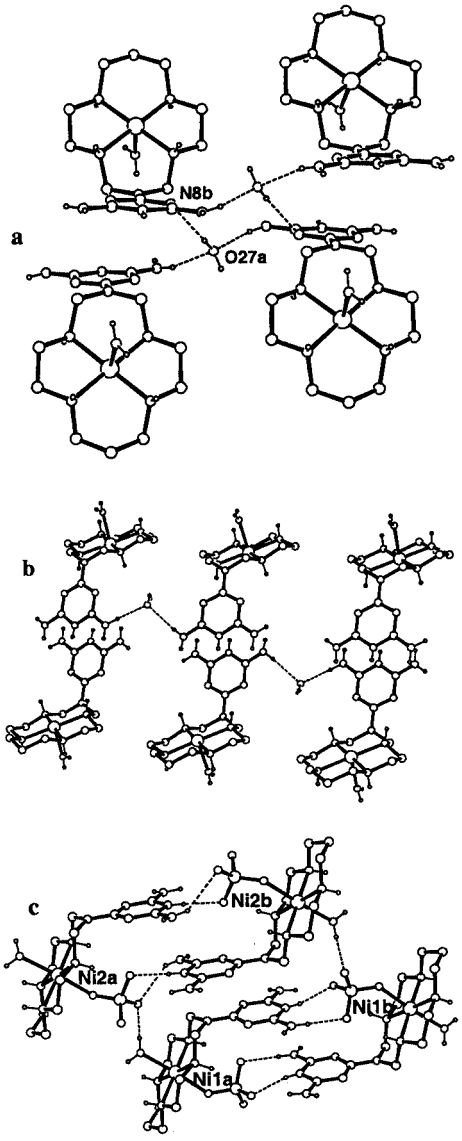

Figure 5. Pair of π-stacked cations (a), modulated tape (b) and modulated π-stacking in the crystal lattice of **3**

interaction plane (see Figure 3a, "open" stack). The only exception is the copper(II) complex **9** for which the π-π interaction plane bisects the metal chromophores (see Figure 3b, "closed" stack).[9] Both "open" [Ni(1a)−Ni(2b) pair] and "closed" stacks [Ni(na)−Ni(nb) pair] are present in the crystal lattice of **3** (Figure 5c), and the sulfate anions have the same dual function as the chloride anions in **9**, i.e., as axial donors they form strong hydrogen bonds to the acceptor centers of the protonated melamine [O(2)···H−N(9′), 2.835 Å; O(3)···H−N(7′), 2.708 Å; O(8)···H−N(19′), 3.114 Å; O(9)···H−N(17′), 2.695 Å]. Also, the stacks in **3** are not isolated and can be considered as modulated, extended chains of π-stacked molecules (see Table 2).

Solution Properties

Electronic Spectroscopy and Equilibria between Diamagnetic and Paramagnetic Compounds

Electronic spectra of the nickel(II) compounds with the mono- and bis(macrocyclic) ligands were measured in nitromethane, acetonitrile and water. The spectra in the UV region are characterized by a strong absorption centered at ca. 210 nm ($\varepsilon \approx 6\ 10^5$ L·mol^{-1}·cm^{-1}), which probably is a superposition of an MLCT band (shoulder at ca. 219 nm) and an intramolecular melamine transition (204 nm in melamine). Absorption spectra in the visible and near-infrared region consist of d-d bands at ca. 330, 455, 660 and > 910 nm, and are typical for nickel(II) complexes of tetraaza-macrocycles and for systems, where nickel(II) complexes with different electronic ground states persist simultaneously in solution [Equations (1) and (2)], i.e., a four-coordinate, planar diamagnetic form (455 nm) and a six-coordinate distorted octahedral paramagnetic form (330, 660 and > 910 nm).[25]

$$[Ni(L)]^{2+} + 2\ solv \rightleftarrows [Ni(L)(solv)_2]^{2+} \quad (1)$$

$$K_{ax} = (\varepsilon_{ls} - \varepsilon_{eff})/(\varepsilon_{eff} - \varepsilon_{hs}) \quad (2)$$

$$\varepsilon_{eff} = \{\varepsilon_{ls}[Ni(L)^{2+}] + \varepsilon_{hs}[Ni(L)(solv)^{2+}]\}/\{[Ni(L)^{2+}] + [Ni(L)(solv)^{2+}]\} \quad (3)$$

In nitromethane there is only a transition at 455 nm for $[Ni(L^1)]^{2+}$ and $[Ni_2(L^2)]^{4+}$, with a molar absorption of 64 L mol^{-1} cm^{-1} per nickel(II) center (see Table 3). Therefore, in the weakly coordinating solvent nitromethane there is no coordination of axial donors, and this allows to determine the molar absorptivity of the diamagnetic form (ε_{ls}). The apparent molar absorption coefficients [ε_{eff}, Equation (3)] of the transition at 455 nm in acetonitrile and aqueous solutions of various electrolytes are lower (see Table 3), indicating the presence of significant amounts of the six-coordinate form in equilibrium with the four-coordinate compounds.

The strength of bonding of axial donors to the nickel(II) centers (increasing K_{ax}, decreasing η) is of similar magnitude for $[Ni(L^1)]^{2+}$ and $[Ni_2(L^2)]^{4+}$ (see Table 3) and significantly higher than for $[Ni(cyclam)]^{2+}$ (cyclam = 1,4,8,11-tetraazacyclotetradecane; 0.1 mol·L^{-1} aqueous $NaClO_4$: $K_{ax} = 0.40$, η = 71%;[26] CH_3CN: η = 22% [27]). An interesting observation is that the thermodynamic parameters for the complexation to axial sites of $[Ni(Me\text{-}azacyclam)]^{2+}$ (Me-azacyclam = 3-methyl-1,3,5,8,12-pentaazacyclotetradecane) are similar to those of the cyclam complex (0.1 mol·L^{-1} aqueous $NaClO_4$: $K_{ax} < 0.5$; CH_3CN: η = 23% [28]), i.e., different to those of the structurally related azacyclam derivatives discussed here. The fact that the spectroscopic properties of all four nickel(II) complexes are similar to each other ($\lambda^{ls}_{max} \approx 455$ nm, $\lambda^{hs}_{max} \approx 330$, 670 and > 900 nm) indicates that metal-centered electronic factors are not the major reason for the drastic differences, and electronic, as well as steric factors related to the capping groups, and differences in solvation may be of importance.

A comparison of the thermodynamic parameters for the axial coordination of water (0.1 mol·L^{-1} $NaClO_4$) to $[Ni(L^1)]^{2+}$ and $[Ni_2(L^2)]^{4+}$ (see Table 3; for details see Supporting Information) with those of $[Ni(cyclam)]^{2+}$ ($\Delta H^0 = -23$ kJ mol^{-1}, $\Delta S^0 = -84$ J mol^{-1} K^{-1}) [29] indicates that the strong axial binding to nickel(II) complexes with the melamine-based ligand is primarily due to an entropy effect (less negative ΔS^0), rather than differences in bond strength (similar ΔH^0). A possible interpretation is that one of the axial water donors [H_2O(A) in Scheme 2] is, upon decomplexation to the four-coordinate form, not released to the bulk solvent, but remains in the first solvation shell. A hydrogen bond similar to that proposed in Scheme 2 was observed in the crystal lattice of **3**.

The largest fraction of the paramagnetic nickel(II) form was observed in the presence of sulfate (see Table 3). There-

Table 3. Effective molar absorptivities (ε, L mol^{-1} cm^{-1}) of the transition at 455 nm of the nickel(II) compounds and equilibria between the diamagnetic and paramagnetic forms in various solvents at 25 °C

Medium	$[Ni(L^1)]^{2+}$			$[Ni_2(L^2)]^{4+}$		
	ε_{eff}	K_{ax}	η (%)[a]	ε_{eff}	K_{ax}	η (%)[a]
CH_3NO_2	64	−	100	128	−	100
CH_3CN	10	10.80	8	21	8.92	9
H_2O; 0.1 mol·L^{-1} $NaClO_4$[b]	23	2.22[c]	28.9	48	2.05[d]	30.5
H_2O; 0.1 mol·L^{-1} $NaNO_3$ [b]	20	2.84	24.2	42	2.61	25.8
H_2O; 0.1 mol·L^{-1} NaCl[b]	19	3.10	22.7	40	2.84	24.2
H_2O; 3.33 10^{-2} mol·L^{-1} Na_2SO_4 [b]	13	6.00	13.3	22	8.15	10.1

[a] Percentage of the diamagnetic form in the equilibrium mixtures, $\eta = (\varepsilon_{eff} - \varepsilon_{hs})/\varepsilon_{ls}$. [b] pH = 7; constant ionic strength. [c] $\Delta H^0 = -23$ kJ mol^{-1}, $\Delta S^0 = -71$ J mol^{-1} K^{-1}. [d] $\Delta H^0 = -21$ kJ mol^{-1}, $\Delta S^0 = -64$ J mol^{-1} K^{-1}.

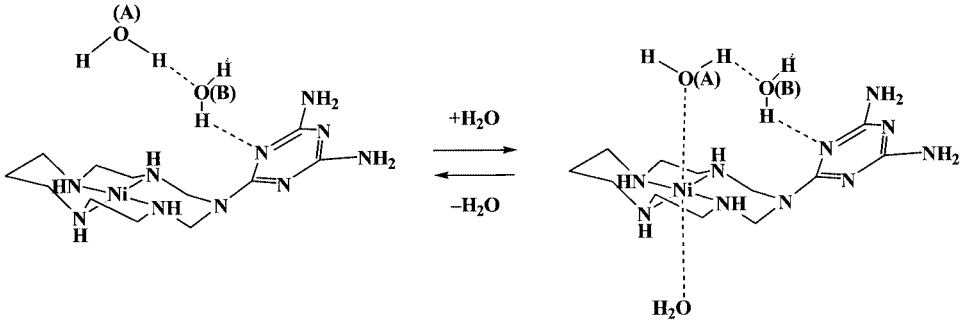

Scheme 2

fore, the stepwise complexation with sulfate was studied in aqueous solution (μ = 0.1 mol·L^{-1}; 0 mol·L^{-1} < [SO_4^{2-}] < 3.33 10^{-2} mol·L^{-1}), see Equation (4), where K_{ax}^{H2O} is the equilibrium constant in absence of sulfate [see Equation (2), 0.1 mol·L^{-1} $NaClO_4$; see Table 3) and K_{ax}^1 to K_{ax}^4 are the stepwise complexation constants with sulfate.

$$K_{ax} = K_{ax}^{H2O} + \sum_{i=1}^{4} [SO_4^{2-}]^i \prod_{j=1}^{i} K_{ax}^i \quad (4)$$

From the data analysis (see Supporting Information) it follows that K_{ax}^2 is ca. 0 for both $[Ni(L^1)]^{2+}$ and $[Ni_2(L^2)]^{4+}$, and fits with higher terms (K_{ax}^3 and K_{ax}^4 for $[Ni_2(L^2)]^{4+}$) do not lead to a significant improvement, i.e., these can be ignored. It emerges that, in sulfate-containing solutions, the mono(sulfate) adduct [per nickel(II) ion] is the primary species, and K_{ax}^1 is significantly larger for $[Ni_2(L^2)]^{4+}$ than for $[Ni(L^1)]^{2+}$ (162 ± 6 L mol^{-1} and 79 ± 10 L mol^{-1}, respectively). Part of this effect may be due to differences in ion pairing [increasing electrostatic attraction with the higher charge of the dinickel(II) complex[30]] but the increasing axial bonding may also be attributed to cooperativity, involving both nickel(II) centers and hydrogen bonding between a coordinated sulfate and an axial water molecule (see Figure 6). Qualitative models suggest that this may lead to stabilization of the sulfate/$[Ni_2(L^2)]^{4+}$ adduct in the *syn* conformation of the dinickel(II) complex.[24] A preliminary structural analysis indicates that in the crystal lattice the dinuclear complex **4** has the *anti* conformation but recent studies on the corresponding copper(II) compounds indicate that the two conformations are similar in energy and that the barrier of interconversion is low.[9,24,31]

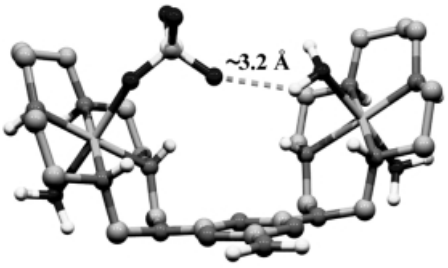

Figure 6. Model for the visualization of cooperativity in the axial bonding of sulfate

Electrochemical Properties and Recognition of Sulfate Anions

The electrochemical behavior of $[Ni(L^1)]^{2+}$ and $[Ni_2(L^2)]^{4+}$ was studied in acetonitrile and aqueous solutions of various salts. In acetonitrile (0.1 mol·L^{-1} [Bu_4N]-ClO_4) a quasi-reversible redox process, assigned to the nickel(III/II) couple is observed {$[Ni(L^1)]$: E_f = 1.084 V (ΔE = 87 mV); $[Ni_2(L^2)]$: E_f = 1.027 V (ΔE = 73 mV)}. An irreversible process {E_{cat} = −1.46 V and −1.40 V for $[Ni(L^1)]^{2+}$ and $[Ni_2(L^2)]^{4+}$, respectively} is attributed to the nickel(II/I) couple; small additional peaks at ca. 0.6 V are assigned to adsorption effects and peaks at ca. 1.3 V may be assigned to ligand oxidation (see Figure 7). The data indicate that both metal centers in $[Ni_2(L^2)]^{4+}$ undergo the redox transformations independently and at the same potentials. Similar results are obtained with [Bu_4N]BF_4 as the electrolyte.

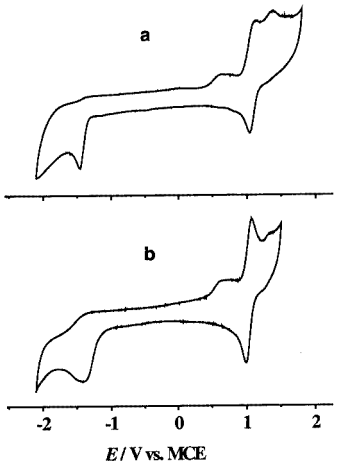

Figure 7. Cyclic voltammograms of 1 10^{-3} mol·L^{-1} solutions of $[Ni(L^1)]^{2+}$ (a) and $[Ni_2(L^2)]^{4+}$ (b) in acetonitrile (0.1 mol·L^{-1} [Bu_4N]ClO_4)

Protonation of non-coordinated nucleophiles in the ligand backbone are known to lead to a destabilization of the oxidized form of metal complexes.[32] As expected, there is approximately an inverse relationship between the destabilization of nickel(III) over nickel(II) and the distance between the nickel center and the site of protonation.[33] For [Ni(Me-azacyclam)] the change of the nickel(III/II) potential upon protonation is ca. 120 mV (0.790 V and

0.910 V in neutral solution and 9.5 mol·L^{-1} $HClO_4$, respectively).[33] The corresponding effects observed for $[Ni(L^1)]^{3+/2+}$ and $[Ni_2(L^2)]^{6+/4+}$ are much smaller (0.815 ± 0.020 V and 0.825 ± 0.010 V, respectively, 10^{-7} mol·L^{-1} < $[H^+]$ < 9.5 mol·L^{-1}). This indicates that, upon protonation of the aromatic fragment, the positive charge is delocalized over the melamine ring.

The electrochemical behavior of $[Ni(L^1)]^{2+}$ and $[Ni_2(L^2)]^{4+}$ in aqueous solution with various electrolytes was studied by cyclic voltammetry (CV) and differential pulse voltammetry (DPV). These data are listed in Table 4, relevant DPV curves of the oxidation scans are collected in Figure 8 and Figure 9. The E_f value for the single quasi-reversible redox transformation of the mono(macrocyclic) ligand complex $[Ni(L^1)]^{2+}$ is strongly anion-dependent and decreases in the order $ClO_4^- > NO_3^- > Cl^- > HSO_4^- \approx H_2PO_4^- > SO_4^{2-} > HPO_4^{2-}$. This sequence is typical for nickel(III/II) couples of azamacrocyclic ligands and reflects the increasing stabilization of nickel(III) by electrostatic effects.[34–36] The poor reversibility observed in the experiments with HPO_4^{2-} is probably related to the high pH of the solutions which leads to a destabilization of the nickel(III) complex with respect to decomposition. This is supported by significantly lower currents observed in the corresponding CV and DPV experiments.

Table 4. Redox potentials (E_f in V vs. MCE, ΔE in mV in parentheses) of the $Ni^{III/II}$ couple of melamine-derived macrocyclic ligand complexes $[Ni(L^1)]^{2+}$ and $[Ni_2(L^2)]^{4+}$ in aqueous solution, containing 0.1 mol·L^{-1} Na^+ salts (CV data, pH = 7.0, sweep rate 0.1 V s^{-1})

Anion of the electrolyte	$[Ni(L^1)]^{2+}$	$[Ni_2(L^2)]^{4+}$
ClO_4^-	0.802 (66)	0.818 (74)
NO_3^-	0.790 (76)	0.794 (78)
Cl^-	0.616 (72)	0.618 (77)
SO_4^{2-}[a]	0.545 (83)	0.488 (62), 0.609 (71)
HSO_4^-[a][b]	0.569 (68)	0.553 (60), 0.638 (60)
$H_2PO_4^-$[c]	0.553 (81)	0.534 (123)[d]
HPO_4^{2-}[e]	0.376 (120)	0.314,[f] 0.428 V[f]

[a] 3.33 10^{-2} mol L^{-1} Na_2SO_4. [b] pH = 1.0 [pK_{a1}(H_2SO_4) = 1.92]. [c] 0.1 mol L^{-1} KH_2PO_4. [d] Sweep rate 0.2 V s^{-1}. [e] pH = 8.2. [f] Anodic peaks of the irreversible oxidation process (DPV).

The behavior of the bis(macrocyclic) ligand complex $[Ni_2(L^2)]^{4+}$ in the presence of perchlorate, nitrate and chloride is similar to that of $[Ni(L^1)]^{2+}$ (see Table 4 and Figure 8). In presence of sulfate or phosphate, however, there are two separate oxidation/reduction steps for $[Ni_2(L^2)]$ (Table 4, Figure 8 and Figure 9). These are reversible in sulfate but only poorly reversible or irreversible in phosphate (similar effects were observed with the mononuclear compound, see above). The fact that the currents for the two-electron oxidation processes in $[Ni_2(L^2)]^{4+}$ in perchlorate-containing solutions are nearly equal to the sum of the two separate single-electron steps in sulfate media indicates that both single-electron oxidation steps are related to the nickel(III/II) couple. Therefore, anion coordination leads to two structurally (and electronically) different nickel centers or to strong coupling of the two metal ions. Also, the reduction potentials of the nickel(III/II) couple in the dinuclear complex are more anodic (E_{f1}) and more cathodic (E_{f2}) than that of the mononuclear compound. For a thorough analysis of the redox processes, the dependencies of the E_f values on the sulfate concentration in neutral (pH = 7.0) and acidic (pH = 1.0) aqueous solutions were studied.

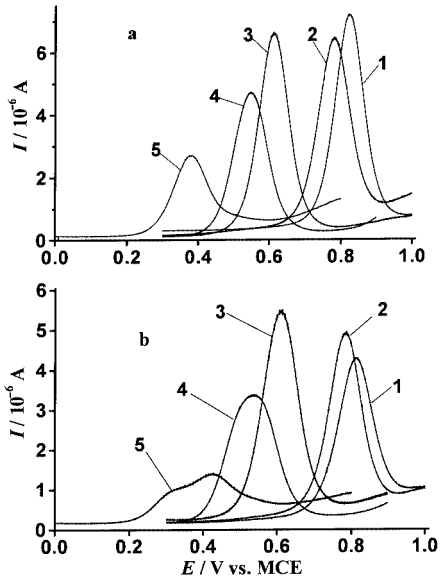

Figure 8. Differential pulse voltammograms of $1.0 \cdot 10^{-3}$ mol·L^{-1} $[Ni(L^1)]^{2+}$ (a) and $5 \cdot 10^{-4}$ mol·L^{-1} $[Ni_2(L^2)]^{4+}$ (b) in 0.1 mol·L^{-1} aqueous solutions of different electrolytes: 1: $NaClO_4$; 2: $NaNO_3$; 3: NaCl; 4: KH_2PO_4; 5: Na_2HPO_4; pulse amplitude 10 mV, potential scan rate 2 mV s^{-1}

The corresponding DPV curves are shown in Figure 9, the potentials are listed in Table 5 (CV curves are given as Supporting Information). The splitting of the redox potential depends on the concentration of the anions and, for a given concentration, it is larger for sulfate than for hydrogen sulfate. The shifts of E_{f1} and E_{f2} are also sensitive to the concentration of the anions. This indicates that sulfate forms adducts of different stability, depending on the nuclearity of the nickel(II) complex. The dependence of the reduction potential of the nickel(III/II) couple on the concentration of the anion X^{n-} is described by Equation (5), where X^{n-} is SO_4^{2-} or HSO_4^-, K_i^{II} and K_i^{III} are the stepwise stability constants of the nickel(II) and nickel(III) complexes with sulfate, and E_f^{aq} is the redox potential in absence of coordinating anions (i.e., in 0.1 mol·L^{-1} aqueous $NaClO_4$). The values of K_i^{II} are relatively small (see above); therefore Equation (5) transforms into Equation (6), where $\Delta E_f = E^X{}_f - E_f^{aq}$.[37]

$$E_f^x = E_f^{aq} - (RT/F) \ln \left(\frac{(1 + \sum_{i=1}^{4} [X^{n-}]^i \prod_{j=1}^{i} K_j^{III})}{(1 + \sum_{i=1}^{4} [X^{n-}]^i \prod_{j=1}^{i} K_j^{II})} \right) \quad (5)$$

$$\exp\{\Delta E_f(-F/RT)\} - 1 = \sum_{i=1}^{4} [X^{n-}]^i \prod_{j=1}^{i} K_j^{III} \quad (6)$$

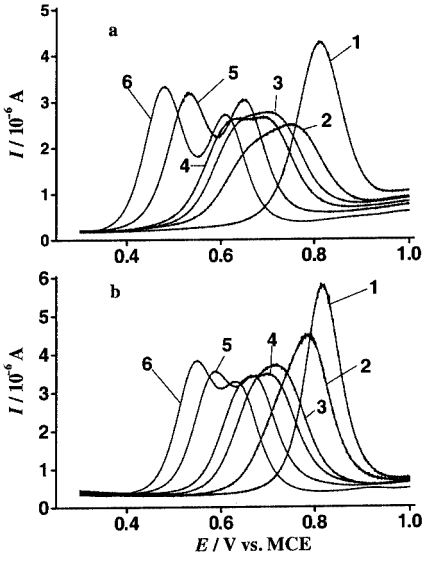

Figure 9. Differential pulse voltammograms of 5.0 10^{-4} mol·L^{-1} $[Ni_2(L^2)]^{4+}$ at various concentrations of Na_2SO_4 (a: pH = 7; 1: 0, 2: 5.0 10^{-4}, 3: 1.0 10^{-3}, 4: 1.5 10^{-3}, 5: 8.7 10^{-3}, 6: 3.3 10^{-2} mol·L^{-1}) and H_2SO_4 (b: pH = 1; 1: 0, 2: 5.0 10^{-4}, 3: 2.4 10^{-3}, 4: 4.6 10^{-3}, 5: 2.5 10^{-2}, 6: 1.0 10^{-1} mol·L^{-1}) (I = 0.1, pulse amplitude 10 mV, potential scan rate 2 mV s^{-1})

Table 5. Parameters of the oxidation of $[Ni_2(L^2)]^{4+}$ in aqueous sulfate solutions

Na_2SO_4 [mol·L^{-1}]	E_{anodic} [V]		$E_{cathodic}$ [V]		E_f [V] (ΔE [mV])	
0.0000	0.855		0.781		0.818 (74)	
0.0005	0.813		0.640		0.727 (173)	
0.0010	0.785		0.605		0.695 (180)	
0.0015	0.755		0.576		0.667 (179)	
0.0024	0.733		0.558		0.646 (175)	
0.0046	0.596	0.708	0.529	0.644	0.563 (67)	0.676 (64)
0.0087	0.573	0.687	0.505	0.619	0.539 (68)	0.653 (68)
0.0153	0.546	0.671	0.482	0.608	0.514 (64)	0.640 (63)
0.0250	0.530	0.658	0.465	0.586	0.498 (65)	0.622 (72)
0.0333	0.519	0.644	0.457	0.573	0.488 (62)	0.609 (71)
H_2SO_4 [mol·L^{-1}]						
0.0000	0.857		0.793		0.825 (64)	
0.0005	0.827		0.732		0.780 (95)	
0.0010	0.803		0.700		0.752 (103)	
0.0015	0.789		0.680		0.735 (109)	
0.0024	0.771		0.658		0.715 (113)	
0.0046	0.751		0.615		0.683 (136)	
0.0087	0.736		0.593		0.665 (143)	
0.0153	0.720		0.569		0.645 (151)	
0.0245	0.619	0.708	0.559	0.648	0.589 (60)	0.678 (60)
0.0630	0.595	0.688	0.535	0.628	0.565 (60)	0.658 (60)
0.1000	0.583	0.668	0.523	0.608	0.553 (60)	0.638 (60)

Plots of E_f^X vs. logC_X, where C_X is the total concentration of SO_4^{2-}, are linear (see Figure 10), and their slopes, divided by 0.059, give the average values of the number of anions coordinated to the metal center involved in the redox transformation (k in Table 6). Interpolation of the dependences of exp{$\Delta E_f(-F/RT)$} vs. C_X, using these values

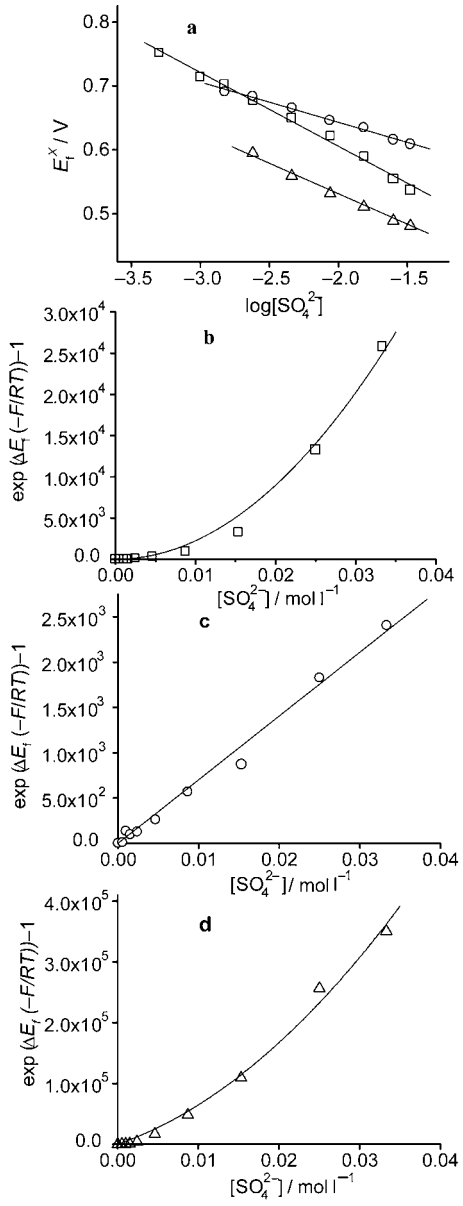

Figure 10. Plots used in the calculations of stoichiometric and thermodynamic parameters for the interaction of sulfate anion with $[Ni(L^1)]^{2+}$ (squares) and those for more anodic (E_{f1}, circles) and less anodic (E_{f2}, triangles) processes observed in $[Ni_2(L^2)]^{4+}$; the curves correspond to best fit lines based on the values presented in Table 6

of k, and assuming that $[SO_4^{2-}] = C_X$ (see Figure 10) allows to obtain values for the corresponding stability constants (see Table 6).

From Table 6 it emerges that the nickel(III) complex with the mono(macrocyclic) ligand forms a bis(sulfate) adduct, although the data analysis did not allow to separate the values of K_1^{III} and K_2^{III}. For $[Ni_2(L^2)]^{6+}$ two separate binding constants for one nickel(III) center (E_{f2}) are observed, the second nickel(III) center (E_{f1}) is coordinated to a single sulfate anion. These results agree well with the model proposed for the explanation of enhanced binding of sulfate to the nickel(II) complex with the bis(macrocyclic) ligand (see electronic spectroscopy, above, Scheme 2). Strong hydrogen

Table 6. Stoichiometric and thermodynamic parameters of the interaction of sulfate with the nickel(III) complexes with the macrocyclic ligands

Anion	$[Ni(L^1)]$	$[Ni_2(L^2)]$ E_{f2}	E_{f1}
SO_4^{2-}	$k = 1.95 \pm 0.01$ $K_1^{III} K_2^{III} = (2.25 \pm 0.02)\cdot10^7$	$k = 1.68 \pm 0.01$ $K_1^{III} = (4.59 \pm 0.02)\cdot10^6$ $K_2^{III} = 41 \pm 10$	$k = 1.06 \pm 0.01$ $K_3^{III} = (7.03 \pm 0.18)\cdot10^4$
HSO_4^-	$k = 1.82 \pm 0.01$ $K_1^{III} = (6.36 \pm 1.05)\cdot10^4$ $K_2^{III} = 28 \pm 10$	$k = 1.83 \pm 0.01$ $K_1^{III} = (2.83 \pm 0.25)\cdot10^5$ $K_2^{III} < 1$	$k = 1.02 \pm 0.01$ $K_3^{III} = (1.19 \pm 0.05)\cdot10^4$

bonding between the coordinated sulfate and an axially coordinated water molecule at the neighboring metal center leads to suppression of the substitution of the remaining water molecule by another sulfate anion. Therefore, one axial coordination site in $[Ni_2(L^2)]^{6+}$ is blocked and two independent reduction processes are observed, one with participation of the bis(sulfate) adduct (E_{f2}) and the other related to the (aqua)(sulfate) complex with the macrocyclic ligand (E_{f1}).

A similar behavior is observed for the nickel complexes in acidic media (pH = 1.0), where hydrogen sulfate is coordinated to the nickel(III) centers (see Table 6). However, the stability constants of the corresponding adducts are significantly lower. This is believed to be due to the smaller charge of the coordinating anion. All constants K_1^{III} for the complexes with the melamine-derived macrocyclic ligands are in the range expected for nickel(III) complexes with tetraaza macrocyclic ligands.[34−36]

Conclusion

The copper(II),[7−9] nickel(II) and nickel(III) complexes of the bis- and tris(macrocyclic) melamine-based ligands are versatile hosts for anionic guest molecules. This is due to the relatively labile coordination to the vacant axial sites, assisted by Jahn−Teller effects [copper(II), nickel(III)] or spin-equilibria [nickel(II)] and to some flexibility in the arrangement of the macrocyclic subunits (*syn-anti* conformations with respect to the melamine rings and relative geometry in the *syn* conformation, angles α, β, γ in Figure 2). In the case of the dinickel(II/III) complexes this leads to an enhanced stability of the coordination of sulfate to one of the axial sites, assisted by the second nickel center. With the di- and trimetal systems [nickel(II), nickel(III), copper(II) and mixed-metal] there is a variety of host systems which, in spite of or due to the limited flexibility are able to selectively bind, activate and/or stabilize anionic guest species.

Experimental Section

Syntheses: ***Caution!*** *Perchlorate salts of metal complexes with organic ligands are potentially explosive and should be handled with care.* $[Ni(2,3,2\text{-tet})](ClO_4)_2$ [2,3,2-tet = bis-*N*,*N*′-(2-aminoethyl)propane-1,3-diamine] was obtained as described,[38] all other AR grade chemicals and solvents were used as received. To a solution of $[Ni(2,3,2\text{-tet})](ClO_4)_2$ (2.0 g, 4.8 mmol) in 15 mL of water were added melamine (1.0 g, 7.9 mmol), triethylamine (5.0 mL, 35.9 mmol) and ethanol (100 mL). The resulting mixture was heated and aqueous formaldehyde (37%, 8.0 mL, 106.7 mmol) was added dropwise over a period of 1 h; refluxing of the solution was continued for an additional 24 h. The mixture was then cooled, and the dark brown precipitate that formed was removed by filtration. The resulting deep brown solution was diluted with water to 2 L and sorbed onto an SP-Sephadex C-25 cation exchange resin (Na^+ form). The column was washed with water (0.5 l) and the products were then eluted with aqueous $NaClO_4$ solutions. Two yellow bands were eluted with 0.2 mol·L^{-1} $NaClO_4$. The first contained unchanged $[Ni(2,3,2\text{-tet})](ClO_4)_2$ and was discarded. With 0.4 mol·L^{-1} $NaClO_4$ a third yellow fraction was obtained. The remaining products were eluted with NaCl or $NaNO_3$ (0.4−0.8 mol·L^{-1}) but did not contain any macrocyclic ligand products.

$[Ni(L^1)](ClO_4)_2\cdot H_2O$ (1): The second yellow band eluted with 0.2 mol·L^{-1} $NaClO_4$ was concentrated under reduced pressure to 25 mL and left cooling to room temperature. Yellow needles of the product were collected, washed with ethanol and dried under vacuum. Yield 0.38 g, 14%. $C_{12}H_{28}Cl_2N_{10}NiO_9$ (586.01): calcd. C 24.60, H 4.82, N 23.90; found C 24.51, H 4.73, N 23.94. Electronic absorption spectrum (H_2O, 0.1 mol·L^{-1} $NaClO_4$): λ_{max} (ε, L mol^{-1} cm^{-1}) = 658 (ca. 2), 455 (23), 330 sh (30), 209 nm (52000). Single crystals of **1**, suitable for X-ray analysis, were selected from the precipitate.

$[Ni(HL^1)](ClO_4)_2Cl\cdot2H_2O$: This complex was obtained with nearly quantitative yield by recrystallization of **1** from 2 mol·L^{-1} HCl. $C_{12}H_{31}Cl_3N_{10}NiO_{10}$ (640.49): calcd. C 22.50, H 4.88, N 21.87; found C 22.45, H 4.83, N 21.67. X-ray quality crystals of $[Ni(HL^1)](ClO_4)_2Cl\cdot H_2O$ (**2**) were obtained by slow concentration of an acidic aqueous solution of **1** containing NaCl.

$[Ni(HL^1)](ClO_4)SO_4\cdot3.5H_2O$: This complex was obtained in nearly quantitative yield by recrystallization of **1** from acidic 1 mol·L^{-1} Na_2SO_4. $C_{12}H_{33}ClN_{10}NiO_{11.5}S$ (627.66): calcd. C 22.96, H 5.30, N 22.32; found calcd. C 23.91, H 5.34, N 22.73. X-ray quality crystals of $[Ni(HL^1)(OSO_3)(OH_2)]_2(ClO_4)_2\cdot5H_2O$ (**3**) were obtained by slow concentration of an acidic solution of **1** containing Na_2SO_4.

$[Ni_2(HL^2)](ClO_4)_5\cdot nH_2O$: The third yellow band which contained the bis(macrocyclic) ligand complex was eluted with 0.4 mol·L^{-1} $NaClO_4$. The volume of the elute was reduced to approximately 25 mL and the hot solution was acidified to pH ≈ 1 with concentrated $HClO_4$ and then cooled. Large orange and small yellow crystals formed were collected, washed with ethanol and dried in air. Total yield: 0.08 g, 1.5%. The crystals were separated manually. Orange complex, $[Ni_2(HL^2)](ClO_4)_5\cdot6H_2O$. $C_{21}H_{59}Cl_5N_{14}Ni_2O_{26}$

Table 7. Crystallographic data for the complexes

	1	**2**	**3**
Empirical formula	$C_{12}H_{28}Cl_2N_{11}NiO_9$	$C_{12}H_{29}Cl_3N_{10}NiO_9$	$C_{12}H_{38}ClN_{10}NiO_{14}S$
Formula mass	586.05	622.51	672.74
Crystal system	monoclinic	triclinic	triclinic
Space group	$P2_1/c$	$P\bar{1}$	$P\bar{1}$
a [Å]	10.8650(14)	8.074(2)	10.9934(6)
b [Å]	8.8691(11)	8.4832(19)	13.6832(7)
c [Å]	23.8863(30)	19.055(4)	18.8799(9)
α [°]	90	93.015(18)	93.9300(10)
β [°]	92.045(3)	93.538(18)	99.8260(10)
γ [°]	90	110.598(18)	96.1030(10)
V [Å^3]	2300.3(5)	1215.5(5)	2771.6(2)
Z	4	2	4
T [K]	190(2)	293(2)	190(2)
$d_{calcd.}$ [g cm^{-3}]	1.692	1.701	1.612
Reflections: measured/unique	13669/4064	3149/2133	46023/16859
$R1$ ($I > 2\sigma$)	0.0536	0.0765	0.0401
$wR2$ (all)	0.1433	0.1843	0.1039
GOF	1.043	1.055	1.027

(1218.42): calcd. C 20.70, H 4.88, N 16.09; found C 20.71, H 4.46, N 15.94. Yellow complex, $[Ni_2(HL^2)](ClO_4)_5\cdot 2H_2O$. $C_{21}H_{51}Cl_5N_{14}Ni_2O_{22}$ (1146.36): calcd. C 22.00, H 4.48, N 17.11; found C 22.06, H 4.65, N 16.78. Recrystallization from nitromethane (diffusion of diethyl ether) of either of these complexes results in the formation of yellow crystals of the composition $[Ni_2(L^2)](ClO_4)_4\cdot 2H_2O$.

$[Ni_2(L^2)](ClO_4)_4\cdot 2H_2O$: $C_{21}H_{50}N_{14}Cl_4Ni_2O_{18}$ (1045.90): calcd. C 24.12, H 4.82, N 18.75; found C 24.05, H 4.77, N 18.63. Electronic absorption spectrum (H_2O, 0.1 mol·L^{-1} $NaClO_4$): λ_{max} (ε, L mol^{-1} cm^{-1}) = 658 (5), 455 (48), 330 (14), 214 nm (62000). Single crystals of $[Ni_2(L^2)](ClO_4)_4\cdot 2H_2O$ (**4**) were grown by vapor diffusion of diethyl ether to a nitromethane solution of $[Ni_2(HL^2)](ClO_4)_5\cdot 2H_2O$.

Crystal Structure Determinations: Reflections of representative crystals were measured with Siemens P4 (**2**) or Bruker AXS SMART 1000 (**1**, **3** and **4**) diffractometers using Mo-K_α radiation (λ = 0.71073 Å) and operating in the ω-scan mode. The structures were solved by direct methods (SHELXS-86) and refined by full-matrix least-squares methods based on F^2 (SHELXL-97),[39] using anisotropic thermal parameters for all non-hydrogen atoms. The crystallographic parameters are given in Table 7. CCDC-172715 (**1**), -172712 (**2**) and -172716 (**3**) contain the supplementary crystallographic data for this paper. These data can be obtained free of charge at www.ccdc.cam.ac.uk/conts/retrieving.html or from the Cambridge Crystallographic Data Centre, 12, Union Road, Cambridge CB2 1EZ, UK [Fax: (internat.) + 44-1223/336-033; E-mail: deposit@ccdc.cam.ac.uk].

Physical Methods: Infrared spectra (KBr pellets) were recorded with a Specord 75 IR (Carl Zeiss) spectrophotometer. Electronic absorption spectra were measured with a Cary1E (Varian) or a Specord M40 (Carl Zeiss) spectrophotometer, equipped with thermostatted cells. The electrochemical experiments (cyclic voltammetry, CV, or differential pulse voltammetry, DPV) were carried out with an Autolab (EcoChemie) system. A standard three-electrode scheme, consisting of a glassy carbon working, a calomel (1 mol·L^{-1} NaCl) reference (MCE) and a Pt plate auxiliary electrode was used. All solutions were purged with argon before measurement. The values of E_f (vs. MCE) for reversible or quasi-reversible redox transformations were calculated as the midpoints between the anodic and cathodic peaks, the distances between peaks (ΔE) were used as parameters for the characterization of the reversibility of the electrochemical transformations (ΔE = 59 mV for thermodynamically reversible process). Analytical data were obtained from the microanalytical laboratory of the chemical institutes of the University of Heidelberg.

Equilibria between Diamagnetic and Paramagnetic Forms: These were measured spectrophotometrically in a thermostatted (± 0.1°) quartz cell (only freshly prepared solutions were used). For aqueous solutions the ionic strength was kept equal at 0.1 mol·L^{-1}; when variable concentrations of sulfate were used the ionic strength was adjusted to 0.1 with $NaClO_4$ and/or $HClO_4$. ε_{ls} = 64 L mol^{-1} cm^{-1} {$[Ni(L^1)]^{2+}$} and 128 L mol^{-1} cm^{-1} {$[Ni_2(L^2)]^{4+}$} were obtained from nitromethane solutions. The ε_{ls} values were obtained from data fitting and Gaussian analyses of the experimental spectra {5 and 9 L·mol^{-1}·cm^{-1} for $[Ni(L^1)]^{2+}$ and $[Ni_2(L^2)]^{4+}$, respectively}. Stability constants for the sulfate adduct formation were calculated by iterative procedures applied to the plots of K_{ax} vs. equilibrium concentrations of sulfate. In a first step the equilibrium concentration of sulfate was assumed to be equal to its total concentration. The values of K^1_{ax} and K^2_{ax} so obtained were then used for the calculation of the equilibrium concentration of sulfate. Iterations were stopped when the difference between two consecutive equilibrium concentrations of the anion was less than $1\cdot 10^{-5}$ mol·L^{-1}.

Acknowledgments

Financial support by the German Science Foundation (DFG), the Committee for Scientific Investigation of Poland and the Foundation of Fundamental Research of the Ministry for Education and Science of the Ukraine are gratefully acknowledged.

[1] A. M. Sargeson, *Coord. Chem. Rev.* **1996**, *151*, 89.
[2] M. P. Suh, *Adv. Inorg. Chem.* **1997**, *44*, 93.
[3] P. Comba, S. M. Luther, O. Maas, H. Pritzkow, A. Vielfort, *Inorg. Chem.* **2001**, *40*, 2335.
[4] R. Bhula, A. P. Arnold, G. J. Gainsford, W. G. Jackson, *Chem. Commun.* **1996**, 143.
[5] O. Costisor, W. Linert, *Rev. Inorg. Chem.* **2000**, *20*, 63.
[6] M. Rossignoli, C. C. Allen, T. W. Hambley, G. A. Lawrance, M. Maeder, *Inorg. Chem.* **1996**, *35*, 4961.

[7] P. V. Bernhardt, E. J. Hayes, *Inorg. Chem.* **1998**, *37*, 4214.
[8] P. V. Bernhardt, E. J. Hayes, *J. Chem. Soc., Dalton Trans.* **1998**, 3539.
[9] P. Comba, Y. D. Lampeka, A. Y. Nazarenko, A. I. Prikhod'ko, H. Pritzkow, *Eur. J. Inorg. Chem.,* in press.
[10] P. Comba, Y. D. Lampeka, L. Lötzberger, A. I. Prikhod'ko, manuscript in preparation.
[11] J.-M. Lehn, *Supramolecular Chemistry: Concepts and Perspectives*, VCH, New York − Weinheim − Basel, **1995**.
[12] D. J. Cram, J. M. Cram, *Container Molecules and Their Guests*, Royal Society of Chemistry, Cambridge, **1994**.
[13] A. Müller, P. Kögerler, *Coord. Chem. Rev.* **1999**, *182*, 3.
[14] D. L. Caulder, K. N. Raymond, *Acc. Chem. Res.* **1999**, *32*, 975.
[15] L. F. Lindoy, I. M. Atkinson, *Self-Assembly in Supramolecular Systems in Monographs in Supramolecular Chemistry*, (Ed.: J. F. Stoddard), Royal Society of Chemistry, Cambridge, **2000**.
[16] E. V. Rybak-Akimova, *Rev. Inorg. Chem.* **2001**, *21*, 207.
[17] S. Aoki, M. Shiro, T. Koike, E. Kimura, *J. Am. Chem. Soc.* **2000**, *122*, 576.
[18] H.-K. Liu, W.-Y. Sun, D.-S. Ma, K.-B. Yu, W.-X. Tang, *Chem. Commun.* **2000**, 591.
[19] M. Ziegler, J. L. Brumaghim, K. N. Raymond, *Angew. Chem. Int. Ed.* **2000**, *112*, 4285.
[20] P. V. Bernhardt, *Inorg. Chem.* **1999**, *38*, 3481.
[21] B. Bosnich, C. K. Poon, M. L. Tobe, *Inorg. Chem.* **1965**, *4*, 1102.
[22] J. C. A. Boeyens, S. M. Dobson, in *Stereochemical and Stereophysical Behaviour of Macrocyclesed*, (Ed.: I. Bernal), Elsevier, Amsterdam, New York, **1987**.
[23] M. Scoponi, E. Polo, F. Pradella, V. Bertolasi, V. Carassiti, P. Goberti, *J. Chem. Soc., Perkin Trans. 2* **1992**, 1127.
[24] P. Comba, T. W. Hambley, N. Okon, G. Lauer, *MOMEC97, a molecular modeling package for inorganic compounds*, CVS Heidelberg, **1997**.
[25] A. B. P. Lever, *Inorganic Electronic Spectroscopy*, 2nd ed., Elsevier Science Publisher, Amsterdam, Oxford, New York, Tokyo, **1984**.
[26] A. Anichini, L. Fabbrizzi, P. Paoletti, R. M. Clay, *Inorg. Chim. Acta* **1977**, *24*, L21.
[27] L. Fabbrizzi, *Inorg. Chim. Acta* **1979**, *36*, L391.
[28] L. V. Tsymbal, S. V. Rosokha, Y. D. Lampeka, *J. Chem. Soc., Dalton Trans.* **1995**, 2633.
[29] L. Sabatini, L. Fabbrizzi, *Inorg. Chem.* **1979**, *18*, 438.
[30] W. G. Jackson, M. L. Hookey, M. L. Randall, P. Comba, A. M. Sargeson, *Inorg. Chem.* **1984**, *23*, 2473.
[31] P. Comba, Y. D. Lampeka, A. I. Prikhod'ko, H. Pritzkow, *Theor. Exper. Chem.* **2001**, *37*, 236
[32] P. S. Pallavicini, A. Perotti, A. Poggi, B. Seghi, L. Fabbrizzi, *J. Am. Chem. Soc.* **1987**, *109*, 5139.
[33] I. M. Maloshtan, PhD Thesis, L. V. Pisarzhevsky, Institute of Physikal Chemistry, Kiev, **1998**.
[34] E. Zeigerson, I. Bar, J. Bernstein, L. J. Kirschenbaum, D. Meyerstein, *Inorg. Chem.* **1982**, *21*, 73.
[35] J. Taraszewska, G. Roslonek, *Supramol. Chem.* **1997**, *8*, 369.
[36] I. Zilbermann, A. Meshulam, H. Cohen, D. Meyerstein, *Inorg. Chim. Acta* **1993**, *206*, 127.
[37] K. V. Gobi, T. Ohsaka, *Electrochim. Acta* **1998**, *44*, 269.
[38] I. M. Maloshtan, S. V. Rosokha, Y. D. Lampeka, *Russ. J. Inorg. Chem.* **1994**, *39*, 759.
[39] G. M. Sheldrick, *SHELXTL 5.1*, Bruker AXS, Madison, WI, **1998**.
[40] C. K. Johnson, *ORTEP, A Thermal Ellipsoid Plotting Program*, Oak National Laboratories, TN, **1965**.

Received March 5, 2002
[I02119]